www.neoplasia.com

Original research

Endogenous hydrogen sulfide regulates xCT stability through persulfidation of OTUB1 at cysteine 91 in colon cancer cells ☆, ☆☆

Shanwen Chen [a]; **Dingfang Bu** [b]; **Jing Zhu** [a];
Taohua Yue [a]; **Shihao Guo** [a]; **Xin Wang** [a];
Yisheng Pan [a]; **Yucun Liu** [a]; **Pengyuan Wang** [a,*]

[a] Division of General Surgery, Peking University First Hospital, Beijing, China
[b] Central laboratory, Peking University First Hospital, Beijing, China

Abstract

Increased xCT and transsulfuration pathway has been associated with metabolic reprogramming of colorectal cancer. However, the correlation between these 2 events and the underlying molecular mechanism remains obscure. xCT expression was determined in tissue microarrays of colorectal cancer. RNA sequencing and functional assays *in vitro* was adopted to delineate the involvement of transsulfuration pathway in the proper function of xCT in maintaining the chemoresistant phenotype. The synthetic lethality of blocking xCT and the transsulfuration pathway was investigated both *in vitro* and *in vivo*. The up-regulation of the transsulfuration pathway after inhibiting xCT in colon cancer cells was evident and exogenous H_2S partially reversed the loss of chemoresistance phenotype after inhibiting xCT. Mechanistically, CTH derived H_2S increased the stability of xCT through persulfidation of OTU domain-containing ubiquitin aldehyde-binding protein 1 at cysteine 91. AOAA and Erastin resulted in synthetic lethality both *in vitro* and *in vivo*, which was mediated through increased ferroptosis and apoptosis. Our findings suggest that a reciprocal regulation exists between xCT and the transsulfuration pathway, which is a targetable metabolic vulnerability. Mechanistically, CTH derived H_2S increased the stability of xCT through persulfidation of OTU domain-containing ubiquitin aldehyde-binding protein 1 at cysteine 91.

Introduction

As the second leading cause of cancer related mortality, colorectal cancer (CRC) remains a hot field in research on targeted cancer therapy. [1] xCT, the functional subunit of system Xc-, imports cystine which upon its conversion to cysteine serves as a precursor for the biosynthesis of glutathione (GSH) [2]. Increased expression of xCT has been related

with the phenotype of chemoresistance and nutrient dependency in multiple types of cancer [3,4]. Immunotargeting xCT with vaccine based on Bovine Herpes virus demonstrated commendable results against breast cancer [5]. Recently, ferroptosis, a newly recognized, iron-dependent form of cell death, has been related with inhibiting xCT in cancer cells [6,7]. Interestingly, increased expression of Cystathionine-β-synthase (CBS), an enzymatic component of transsulfuration pathway, was evident in cells with resistance to ferroptosis induced by Erastin, a common used inhibitor of xCT [8]. The transsulfuration pathway together with the methionine cycle, acts as an important source of endogenous cysteine, especially in the ablation of xCT mediated extracellular source of cysteine [9]. CBS has also been confirmed as an independent regulator of ferroptosis [10,11]. Cysteine, imported by xCT, is a substrate for CBS and cystathionine-γ-lyase (CTH) in the transsulfuration pathway to produce hydrogen sulfide (H_2S) [12]. Endogenous H_2S, a byproduct of the transsulfuration pathway and the third confirmed gaseous transmitter, is intimately involved in tumor cell physiology and under delicate regulation in multiple types of cancer [13,14].

462 Endogenous hydrogen sulfide regulates xCT stability through persulfidation of OTUB1 at cysteine 91 in colon cancer cells **S. Chen et al.**

Neoplasia Vol. 23, No. xxx 2021

Recently, persulfidation of cysteine residues mediated by endogenous H_2S has been reported by accumulating studies as an important post-translational modification of proteins [15,16]. However, the interplay between xCT and the transsulfuration pathway and the targeting value of combined blocking of these 2 events remains elusive.

In the current study, we explored the reciprocal regulation between xCT and the transsulfuration pathway and the involvement of this interplay in the chemoresistance and ferroptosis of colon cancer cells. Our data demonstrated that xCT downregulation induced decreased endogenous H_2S levels and increased expression of CTH, a major enzymatic component of the transsulfuration pathway. Besides, endogenous H_2S, derived from the transsulfuration pathway, increased the stability of xCT through persulfidation of OTU domain-containing ubiquitin aldehyde-binding protein 1 (OTUB1) at cysteine 91. The reciprocal regulation between endogenous H_2S and the stability of xCT led to the investigation of the potential of targeting these 2 events in CRC and the results revealed a synthetic lethal effect of combining AOAA and Erastin both *in vitro* and *in vivo*.

Materials and methods

Cell lines and culture

Human colorectal cancer cell lines (HCT-116 and HT-29) were obtained from American Type Culture Collection and cultured in McCoy's 5A supplemented with 10% fetal bovine serum and antibiotics (100 U/ml penicillin and 0.1 mg/ml streptomycin) at 37°C with 5% CO_2 in a humidified atmosphere. All the cell lines were tested for mycoplasma contamination before use and validated by short tandem repeat profiling.

Lentivirus, plasmids and siRNA transfection and selection of stable transfection cell lines

Cells were transduced with lentiviruses containing shRNA sequences targeting CTH and xCT (shCTH: Sigma-Aldrich SHCLNV, clone TRCN0000416390; shxCT: Sigma-Aldrich SHCLNV, clone TRCN0000043123. A non-targeting control shRNA sequence was used as negative control. Colon cancer cells were infected at a MOI of 3 with hexadimethrine bromide (8 μg/ml). Puromycin (4ug/ml) were added 3 d after transfection and clones with stable transfection were collected. The plasmid pcDNA 3.1 –OTUB1 (Keap1-WT) was purchased from Vigenebio (China). Successful point mutation of Cysteine23, Cysteine91, Cysteine204, or Cysteine 212 to alanine was confirmed by DNA sequencing. The expression plasmids were transfected into cells with Lipofectamine 3000 reagent (Thermofisher, USA). SiRNAs targeting CTH, OTUB1 and the scrambled negative control RNAs were purchased from GenePharma (China).

Tissue microarrays and immunohistochemistry (IHC) analysis

Tissue microarrays (CO1801) containing 90 CRC cancer tissues and paired adjacent normal tissues were purchased from US Biomax and IHC analysis of xCT was performed utilizing rabbit anti-xCT antibodies (Abcam, UK). Another set of specimens composed of 19 paired primary CRC and liver metastasis (LM) sites were collected and analyzed at the Peking University First Hospital with written informed consent.

RNA extraction and real-time PCR

Total RNA isolation and cDNA synthesis were performed with Trizol (Thermofisher, USA) and RevertAid First Strand cDNA Synthesis Kit (Thermofisher, USA). Quantitative real-time PCR analysis was performed with 7500 real-time PCR System (Applied Biosystems). RNA relative expression was calculated as fold change using the comparative threshold cycle (CT) method ($2^{-\Delta\Delta CT}$) with GAPDH serving as the internal control. The primers are listed in the supplementary Table S1.

Detection of H_2S levels

A fluorescent probe of H_2S, kindly provided by Professor Long Yi from Beijing University of Chemical Technology, was utilized to visualize endogenous H_2S in cells and photos were taken under CarlZeiss LSM710 confocal microscope (CarlZeiss, German) [17]. H_2S levels in tumor tissues were determined as previously described [18]. Briefly, tumor tissues were lysed and protein concentration was determined by BCA method. Lysates were incubated with a reaction mixture containing pyridoxal-5-phosphate (2 mM) at 37°C for 30 min. Next, trichloroacetic acid solution (10%) was added to each sample followed by zinc acetate (1%). Then, N,N-dimethyl-p-phenylendiamine sulfate (DPD, 20 mM) in HCl (7.2 M) and $FeCl_3$ (30 mM) in HCl (1.2 M) were added, and the absorbance of the solutions was measured at a wavelength of 650 nm. H_2S production was plotted against a standard curve generated by serial dilution of NaHS.

RNA sequencing

Total RNA was extracted and purified using a TRIzol reagent kit (Thermofisher, USA) and Oligo (dT)-attached magnetic beads were used to purified mRNA. Purified mRNA was fragmented into small pieces with fragment buffer and the first-strand cDNA was generated in First strand reaction system by PCR, and the second-strand cDNA was generated as well. The reaction product was purified by magnetic beads. The cDNA fragments with adapters were amplified by PCR, and the products were purified by Ampure XP Beads. The library was assessed quality and quantity using the Agilent 2100 bioanalyzer. Then, undergo DSN treatment. The DSN treated library was assessed quality to ensure the high quality of the sequencing data by 2 methods: checked the distribution of the fragments size using the Agilent 2100 bioanalyzer, and quantified the library using real-time quantitative PCR (qPCR). The qualified library was amplified on cBot to generate the cluster on the flowcell. And the amplified flowcell was sequenced single end on the HiSeq4000 platform (BGI-Shenzhen, China).

Western blotting

Proteins extracts were analyzed by western blotting following standard protocols with primary antibodies specific for xCT (ab37185, Abcam), CBS (#14782, CST), CTH (#60234-1-Ig, Proteintech), MPST (sc-376168, Santa cruz), GAPDH (#5174, CST), OTUB1 (#3783, CST), CD44s (ab185924, Abcam), PARP (#9532, CST), Cleaved PARP (#5625, CST), Caspase 3 (#9662, CST) and Cleaved Caspase 3 (#9664, CST). Images were collected utilizing Syngene GeneGenius gel imaging system (Syngene, UK) following the manufacturer's instructions.

Immunoprecipitation (IP)

IP was performed with xCT antibodies (ab37185, Abcam) and Pierce Protein A/G Magnetic Beads following the manufacturer's recommendations. Briefly, 50 μl of magnetic beads was incubated with control or xCT antibodies (1μg) overnight at 4°C with constant rotation. Cell lysates were incubated with antibody-conjugated beads for an additional 12 h. After incubation, beads were washed and the precipitated proteins were eluted with loading buffer and boiled for 10 min at 99°C. The supernatants were subjected to SDS-PAGE followed by immunoblotting with specific antibodies.

Colony formation assays (CFA)

Forty-eight hours after transfection with siRNAs, cells were seeded into 6-well plates at density of 1000 cells per well and incubated with indicated doses of 5- fluorouracil (5-FU) for 2 wk. After fixation with 4% formaldehyde, cells were stained with 0.05% crystal violet for 2 min at room temperature, followed by washing with PBS and drying.

Cell viability assays

Cellular activity was tested by the CCK-8 assay (Beyotime, China). Briefly, 5000 cells were added to each well of a 96-well plate (Corning, USA). Cells were treated with gradient concentrations of 5-FU, AOAA, SAS, or Erastin for 48 h and the IC50 values of corresponding reagents were measured. Combination index was calculated with Chou-Talalay method as described previously [19].

Cycloheximide chase assays

Cycloheximide chase assays were performed as described previously [20]. Briefly, 48 h after transfection with siRNAs or 24 h after pretreatment with AOAA and Erastin, cells were treated with $30\mu g/ml$ cycloheximide (#66-81-9, Sigma-Aldrich) for indicated times and lysed for immunoblotting analysis.

Modified Biotin switch assay of persulfidation

A modified biotin switch assay was performed utilizing a biotin switch assay kit (ab236207, Abcam) with little modifications [21]. Briefly, cell or tissue samples were homogenized in HEN buffer (250 mM HEPES-NaOH [pH 7.7] supplemented with 1 mM EDTA and 0.1 mM neocuproine) containing 150 μM deferoxamine, 1% Nonidet-P40 (NP-40), and protease/phosphatase inhibitors. The homogenized samples were sonicated and centrifuged at $13000 \times g$ for 20 min at $4°C$. The lysates were added to HEN buffer supplemented with 2.5% SDS and 20 mM methyl methanethiosulfonate (MMTS). The samples were frequently shaken at $50°C$ for 30 min. Then, the MMTS was removed by adding acetone and the samples were precipitated at $-20°C$ for 1 h. The pellets were suspended in HEN buffer containing 1% SDS and 4 mM biotin-HPDP. After 3 h of incubation at $25°C$, the proteins were purified with acetone. Finally, the proteins were dissolved in solution buffer, purified with streptavidin–agarose beads and subjected to western blotting with an anti-OTUB1 antibody (#3783, CST). Cells treated by dithiothreitol (DTT) (1 mmol/L) served as negative control group.

Immunofluorescence (IF)

Cells cultured on coverslips were rinsed with PBS and fixed by 100% acetone at $-20°C$ for 1 min. Coverslips were then rinsed in PBS followed by blocking with 1% bovine serum albumin for 2 h at room temperature. Subsequently, coverslips were incubated with $5\mu g/mL$ rabbit monoclonal anti-xCT antibody (ab37185, Abcam) overnight at $4°C$. After being washed with PBS, coverslips were incubated with goat anti-rabbit immunoglobulin conjugated to Alexa488 (1:300 dilutions; #A-11034, Thermofisher) in 1% bovine serum albumin for 1 h at room temperature. After being washed with PBS, coverslips were mounted using ProLong™ Gold Antifade Mountant with DAPI reagent (P36935, Thermofisher) and stored at $4°C$ in dark until analyzed. The fluorescence was visualized under LSM710 confocal microscope (Carl Zeiss).

Tumorigenesis in nude mice

This study has been approved by the institute review board at Peking University First Hospital (No. 202030) and performed in accordance with the Helsinki Declaration. Male BALB/c nude mice (3 wk old) were purchased from Vital River (Beijing, China) and raised in the containment unit of the Laboratory Animal Center at the Peking University First Hospital. Mice were allowed to adapt to the environment for 1 wk before any treatment. HCT-116 cells (10^6 cells/mouse, 0.2 ml DMEM) were subcutaneously injected into the flank fat pads of 4-wk-old male nude mice. Five days later when the xenografts were palpable, mice were randomly assigned to 1 of 4 groups and subjected to IP injection: control (PBS), AOAA (5 mg/kg in PBS, 5 d per wk), Erastin (10 mg/kg in PBS, 5 d per wk), and Erastin+AOAA. Tumor volume was monitored every 3 d according to the following formula: tumor volume (mm^3) $= 4\pi xyz/3$, where 2x, 2y, and 2z represent 3 perpendicular diameters of the tumor. After 30 d, mice were anaesthetized with diethyl ether and sacrificed by cervical dislocation and xenografts were harvested.

GSH assays

The reduced GSH concentration in cell lysates was measured by using the Reduced Glutathione (GSH) Assay kit (#K464-100, BioVision) following the manufacturer's instructions. The results were normalized to total protein concentrations.

Malondialdehyde (MDA) assays

The MDA concentration in tumor tissues was measured by using the Lipid Peroxidation (MDA) Assay Kit (Colorimetric/Fluorometric) (ab118970, Abcam) following the manufacturer's recommendations. The results were normalized to total protein concentrations.

Statistical analysis

All the data are presented as means with their standard error of the mean (means + SEM). Analyses were performed by using GraphPad Prism Software 8.0 (San Diego, CA, USA). Student t test were used for 2 groups, and One-way ANOVA was applied for comparing more than 2 groups. A $P < 0.05$ was used to indicate statistical significance.

Results

Increased expression of xCT and the up-regulation of the transsulfuration pathway after inhibiting xCT in colon cancer cells

A tissue microarray composed of 90 CRC tissues and paired adjacent normal tissues was initially utilized to analyze the expression of xCT and the results indicated a significantly increased expression of xCT in CRC tissues (Fig. 1A). IHC analysis of samples collected from 19 primary CRC tissues and paired LM sites further indicated an increased expression of xCT in the LM sites, indicating a potential role of xCT in the process of LM (Fig. 1B). Colon cancer cell lines with acquired resistance to 5-FU were developed from parental HT-29 and HCT-116 cell lines by increasing doses of exposure and the overexpression of xCT in both protein and mRNA levels were evident in cell lines with acquired resistance to 5-FU (Fig. 1C). Considering the role of intracellular cysteine, imported by xCT, as a major source of synthesis of H$_2$S, we propose that xCT might be involved in the regulation of endogenous H$_2$S levels. Not surprisingly, we observed significantly increased H$_2$S levels in both 5-FU resistant cell lines (Fig. 1D). Analysis of TCGA database also revealed increased expression of xCT mRNA in colon cancer tissues and increased expression of xCT together with another subunit of system Xc-, SLC3A1, was
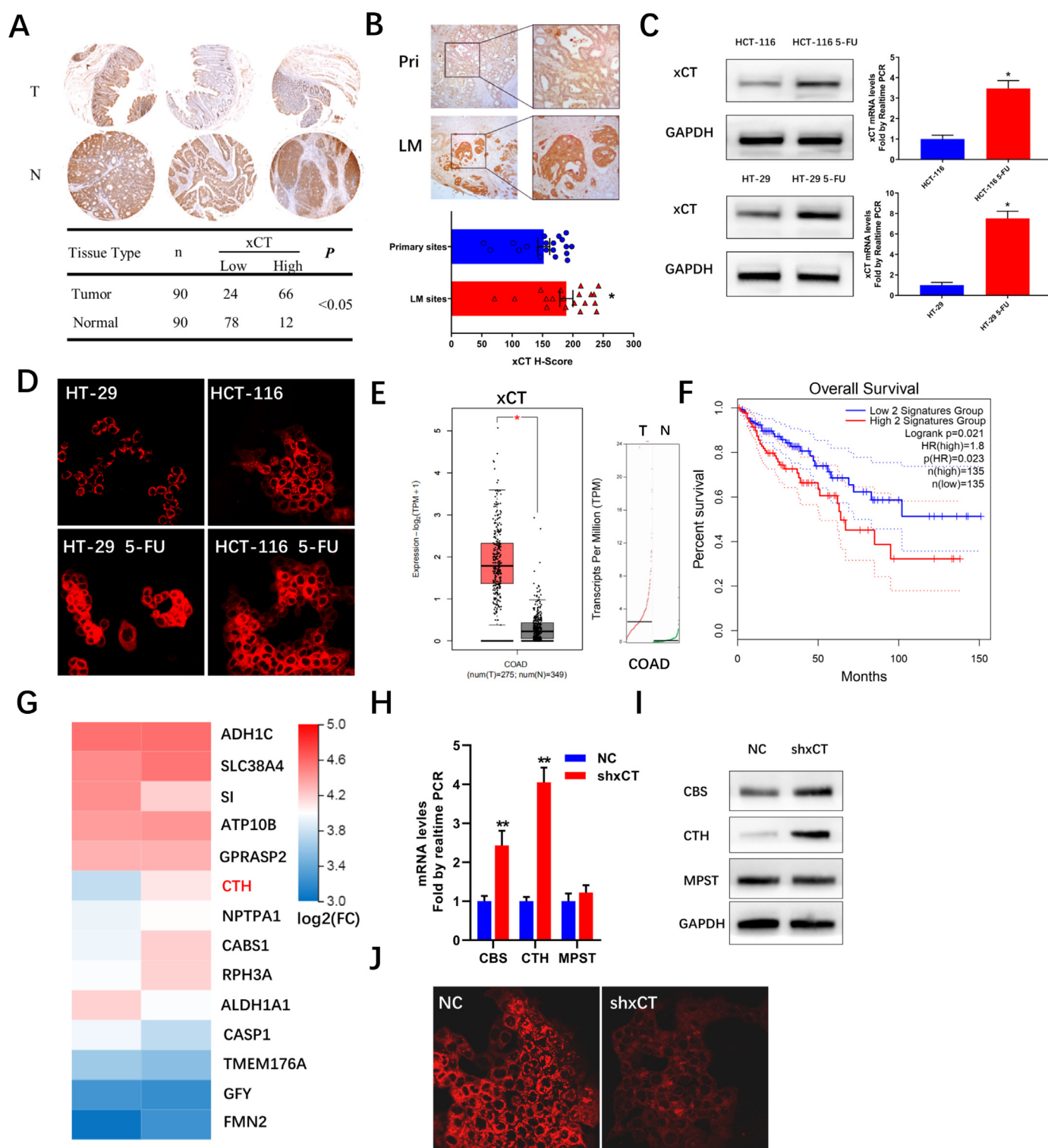
Fig. 1. Increased expression of xCT in CRC and 5-FU resistance. (A) IHC analysis of xCT expression in tissue microarray composed of 90 CRC and paired adjacent normal tissues. (B) Representative images and results of IHC analysis of xCT expression in 19 paired primary and LM sites. (C) Immunoblot and mRNA results showing increased expression of xCT in 5-FU resistant cells. (D) H_2S fluorescent probe indicating increased H_2S levels in 5-FU resistant cells. (E) GEPIA online analysis showing significantly higher expression of xCT was observed in tumor patients (N = 275) compared with healthy controls (N = 349) in TCGA database. (F) High expression of xCT together with SLC3A2 is associated with a decrease in overall survival in CRC patients. (G) Leading upregulated genes after xCT knockdown in HCT-116 cells. (H) and (I) Quantitative real-time PCR and immunoblot images showing increased CBS and CTH levels in HCT-116 cells with xCT knockdown. J, H_2S fluorescent probe indicating decreased H_2S levels in HCT-116 cells with xCT knockdown. (*P < 0.05, ** P < 0.01)

related with worse prognosis in CRC (Fig. 1E and F). HCT-116 cell lines with stably decreased expression of xCT was constructed with shRNA and RNA sequencing was further performed to investigate the role of xCT in CRC. Surprisingly, CTH, the rate-limiting enzyme in the transsulfuration pathway as well as a major producer of H_2S, was among the leading up-regulated genes in cells with decreased expression of xCT (Fig. 1G). We further analyzed the expression of CBS, CTH and MPST, which were the producers of H_2S in colon cancer cell lines, and the results revealed increased expression of both CBS and CTH, not MPST, in both protein and mRNA levels after inhibiting xCT in HCT-116 cell lines (Figs 1H and I). CBS and CTH are the enzymatic components of transsulfuration pathway with H_2S as a byproduct of this process. A H_2S fluorescent probe was adopted to investigate the intracellular H_2S levels and the results indicated decreased H_2S levels after inhibiting xCT in HCT-116 cells (Fig. 1J). Considering the pivotal role of both xCT and transsulfuration pathway in the metabolism of cancer cells, we set out to investigate the correlation and targetable potential between these 2 events.

xCT regulates endogenous H_2S levels and CTH-H_2S axis stabilizes xCT

SiRNAs were utilized to inhibit the expression of xCT or CTH in colon cancer cell lines and their efficacy was validated by western blotting (Fig. 2A). CFA assays indicated that both xCT and CTH contributed to the phenotype of 5-FU resistance in colon cancer cells, which was also in accordance with IC50 assays (Figs. 2B and C). xCT and transsulfuration pathway were 2 major sources of cysteine, which was the limiting precursor in the synthesis of GSH [22]. Indeed, both inhibiting xCT and CTH decreased GSH levels (Fig 2D). We further tested H_2S levels, a byproduct of transsulfuration pathway, and the results indicated decreased endogenous H_2S after inhibiting xCT and CTH (Fig. 2E). These results reveal a regulatory effect of both xCT and CTH on the endogenous H_2S levels. We further set out to investigate the effect of H_2S on the attenuation of 5-FU resistance induced by xCT inhibition. Surprisingly, GYY4137, a slow releasing donor of H_2S [23], saved the 5-FU resistant phenotype from xCT inhibition, demonstrating a functional role of H_2S in the cancer-promoting effect of xCT (Figs. 2F and G). GYY4137 also significantly alleviated the decreased GSH values induced by interfering xCT (Fig. 2H). We further tested the effect of the CTH-H_2S axis on the expression of xCT and the results indicated that CTH inhibition induced decreased levels of xCT protein, which was ameliorated by GYY4137 (Fig. 2I). What's more intriguing was that neither inhibiting CTH with siRNA nor GYY4137 exerted an effect on xCT mRNA levels (Fig. 2J). These results indicated that CTH-H_2S axis might regulate the xCT levels in post-translational levels.

CTH derived H_2S persulfidates OTUB1 at cysteine 91 to regulate its binding with xCT

Cyclohexamide chase assay is a classical method for detecting protein stabilization and the results indicated that inhibiting CTH dramatically decreased the stability of xCT in HCT-116 cells, which was ameliorated by GYY4137 (Fig. 3A). These results indicated that a reciprocal regulation between xCT and CTH-H_2S axis might exist. Persulfidation of specific cysteine residues has been reported to be a wide spread modification of proteins mediated by H_2S [24]. OTUB1, a deubiquitinase, has been reported to be involved in the regulation of xCT stability by directly conjugating with xCT and CD44s [25]. The amino acid sequence data of OTUB1 was obtained from Uniprot and 4 cysteine residues (C23, C91, C204, C212), which might be targets for persulfidation mediated by H_2S, were identified. We further adopted the modified biotin-switch assays to investigate the persulfidation of OTUB1 and the results indicated that inhibiting CTH with siRNA decreased the persulfidation of OTUB1, which was ameliorated by GYY4137 (Fig. 3B). IPs with xCT antibodies were further performed to investigate the regulatory effect of persulfidation of OTUB1 on its conjunction with xCT and the results indicated that inhibiting CTH

decreased the conjunction of OTUB1 with xCT and CD44s as well as decreased the protein levels of xCT, which was ameliorated by GYY4137 (Fig. 3C). The results of IF of xCT was in accordance with IP and western blotting, further indicating the regulatory role of CTH-H_2S on the steady state levels of xCT (Fig. 3D). To delineate the essential cysteine residues for the regulatory effect of H_2S on the conjunction of OTUB1 with xCT, we further constructed OTUB1 expressing plasmids with point mutation from cysteine to alanine (C23A, C91A, C204A and C212A). Biotin switch assays indicated that none of these plasmid alone could abrogate the persulfidation of OTUB1 mediated by H_2S, indicating that H_2S persulfidates OTUB1 at multiple cysteine residues (Fig. 3E). Small interfering RNAs targeting the 3'UTR region of OTUB1 mRNA was constructed to rule out the influence of endogenous OTUB1, while at the same time retaining the expression of exogenous OTUB1 expressing plasmids. Biotin switch assays following co-transfection suggested that C91A, instead of other 3 plasmids, abrogated the increase of xCT levels induced by GYY4137 (Fig. 3F). GYY4137 induced increased conjunction of OTUB1 with xCT in cells transfected with OTUB1siRNA and OTUB1 C23A expressing plasmids (Fig. 3G). However, C91A expressing plasmids abrogated the increased conjunction of OTUB1 with xCT and CD44s induced by GYY4137 (Fig. 3H). Together, these results indicated that endogenous H_2S could increase the binding of OTUB1 with xCT by persulfidating OTUB1 at cysteine 91 to regulate the stability of xCT.

Synthetic lethality of blocking xCT and transsulfuration pathway in colon cancer cells

The reciprocal regulation between xCT stability and transsulfuration derived H_2S led us to investigate the potential of targeting these 2 events at the same time. AOAA, an inhibitor of pyridoxal phosphate -6 dependent enzymes including both CBS and CTH, was adopted to targeting the transsulfuration pathway [26]. Both sulfasalazine (SAS) and Erastin were adopted to targeting the activity of xCT. Synergistic effect of AOAA with both SAS and Erastin was noticed in inhibiting the viability of both HCT-116 and HT-29 cells, with more pronounced effect of combing AOAA and Erastin, featured by smaller combination indexes (Figs. 4A and B). The combination of AOAA and Erastin was adopted in the following assays. The results indicated that combing AOAA and Erastin significantly exaggerated the decreased GSH levels as well as increased expression of PTGS2 and MDA levels, which were widely accepted markers of ferroptosis (Figs 4C, D and E). Elevated cleavage of both PARP and Caspase 3 indicated that increased apoptosis might also be involved in the synthetic lethality induced by this combination (Fig 4F). The results of IF validated further decreased xCT and endogenous H_2S levels induced by this combination (Figs 4G and H). This combination resulted in further decreased persulfidation of OTUB1 compared with either AOAA or Erastin alone (Fig. 4I). Besides, IPs indicated decreased levels of xCT and decreased conjunction between OTUB1 and xCT after incubation with this combination (Fig. 4J). Cyclohexamide chase assays revealed drastically decreased stability of xCT following incubation with this combination (Fig. 4K). Together, these results indicated the synthetic lethality of targeting xCT and the transsulfuration pathway through adopting AOAA and Erastin in colon cancer cells.

In vivo validation of H_2S mediated persulfidation of OTUB1 and synthetic lethality

Subcutaneous tumor growth assays were performed after inhibiting the expression of CTH (Fig. 5A). Decreased growth rate was noticed in cells with stably decreased expression of CTH (Fig. 5B). IHC analysis indicated decreased expression of xCT and inhibited proliferation marker proliferating cell nuclear antigen (PCNA) intensity in shCTH tumors (Fig. 5C). Decreased H_2S levels and decreased persulfidation of OTUB1 was evident in shCTH groups (Figs. 5D and E). Besides, inhibiting CTH resulted in decreased
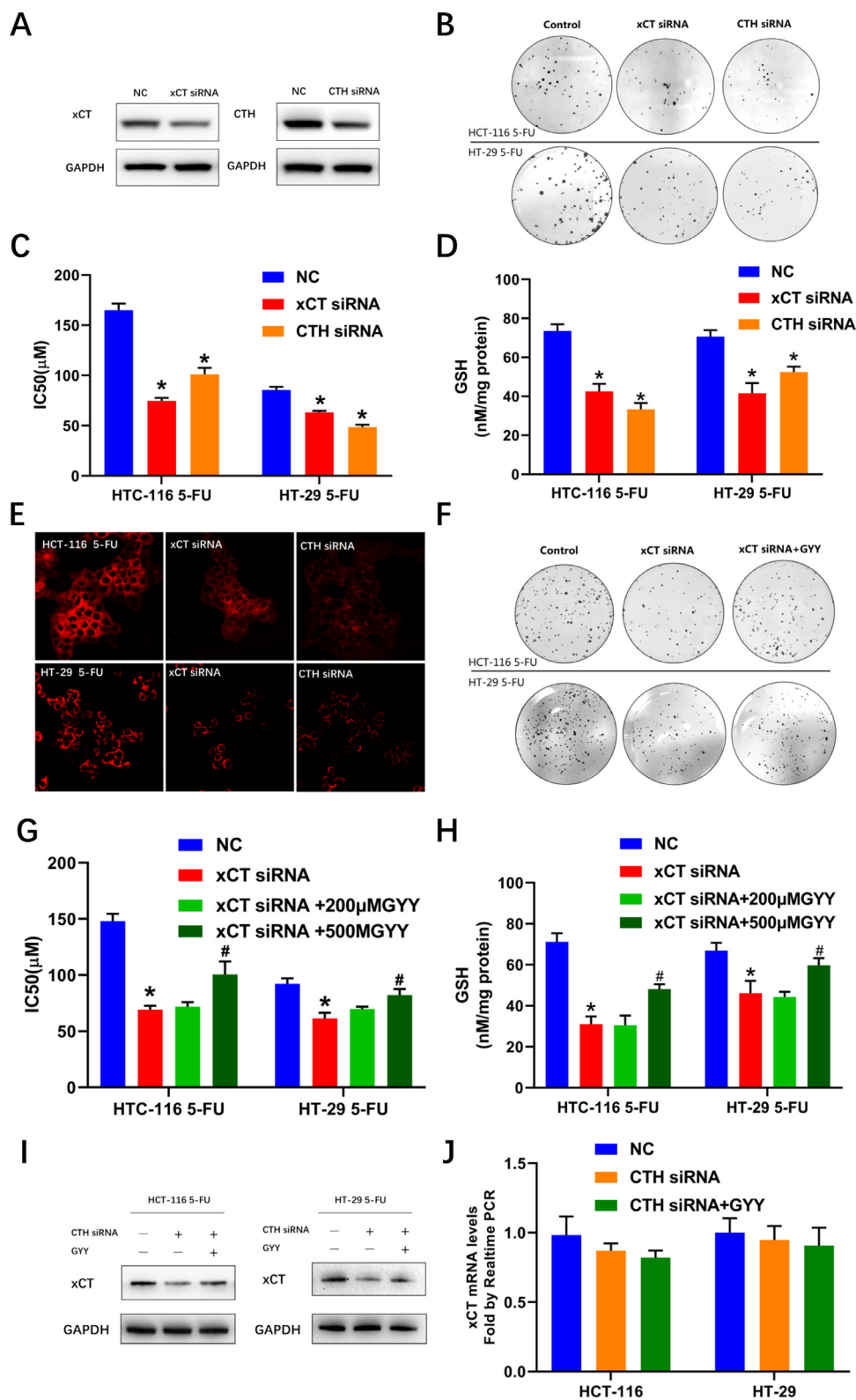
Fig. 2. CTH-H_2S contributes to the 5-FU resistance maintained by xCT overexpression. (A) immunoblots showing inhibiting the expression of xCT or CTH using specific siRNAs. (B) Interfering xCT or CTH expression inhibited clonogenicity of both colon cancer cell lines in the presence of 5-FU. (C) IC50 values of 5-FU after inhibiting xCT and CTH expression in both cell lines. (D) GSH values after inhibiting xCT and CTH expression in both cell lines. (E) H_2S fluorescent probe indicating decreased H_2S levels in both cell lines after inhibiting xCT or CTH. (F) GYY4137 saved the attenuated clonogenicity in both cell lines after inhibiting xCT. (G) and (H) GYY4137 saved the decreased IC50 of 5-FU and GSH values after inhibiting xCT in both cell lines. (I) GYY4137 promoted the attenuated levels of xCT after inhibiting CTH expression with siRNAs. (J) Quantitative real-time PCR showing no effect of either inhibiting CTH or GYY4137 on xCT mRNA levels. (* $P < 0.05$ vs negative control [NC], #$P < 0.05$ vs xCT siRNA groups)
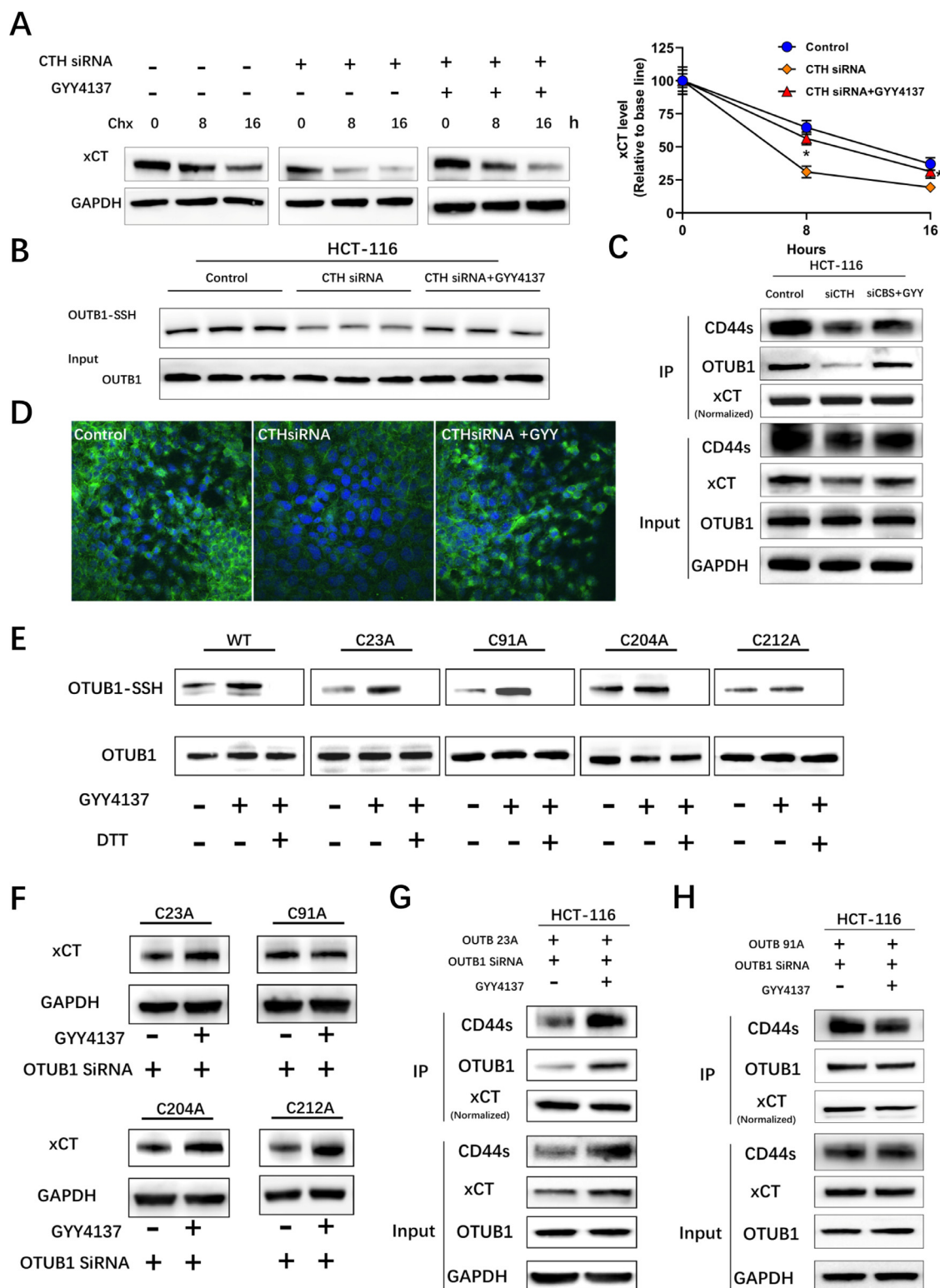
Fig. 3. H_2S improves the stability of xCT through persulfidation of OTUB1 at cysteine 91. (A) Cycloheximide chase assays showing decreased stability of xCT after inhibiting xCT, which was ameliorated by $500\mu M$ GYY4137 (* $P < 0.05$ vs CTH siRNA). (B) Modified biotin switch assays showing decreased persulfidation of OTUB1 after inhibiting xCT, which was ameliorated by GYY4137. (C) Immunoblots following IP showing decreased expression of xCT and decreased conjunction between xCT and OTUB1 after inhibiting CTH in HCT-116 cells, which was ameliorated by GYY4137. (D) IF of xCT indicating decreased xCT expression after inhibiting xCT, which was ameliorated by GYY4137. (E) Modified biotin switch assays showing no effect of these expressing plasmids on the persulfidation mediated by GYY4137 in HCT-116 cells, dithiothreitol (DTT) treated samples served as negative controls. (F) Immunoblots showing that OTUB1 C91A expressing plasmids abrogated the increased xCT levels induced by GYY4137 in HTC-116 cells transfected with exogenous OTUB1 expressing plasmids and OTUB1 siRNAs. (G) Immunoblots after IP showing no effect of OTUB1 C23A plasmids on the increased persulfidation and increased conjunction between OTUB1 and xCT induced by GYY4137. (H) OTUB1 C91A plasmids abrogated the increased persulfidation and increased conjunction between OTUB1 and xCT induced by GYY4137.

468   Endogenous hydrogen sulfide regulates xCT stability through persulfidation of OTUB1 at cysteine 91 in colon cancer cells   S. Chen et al.

Neoplasia Vol. 23, No. xxx 2021
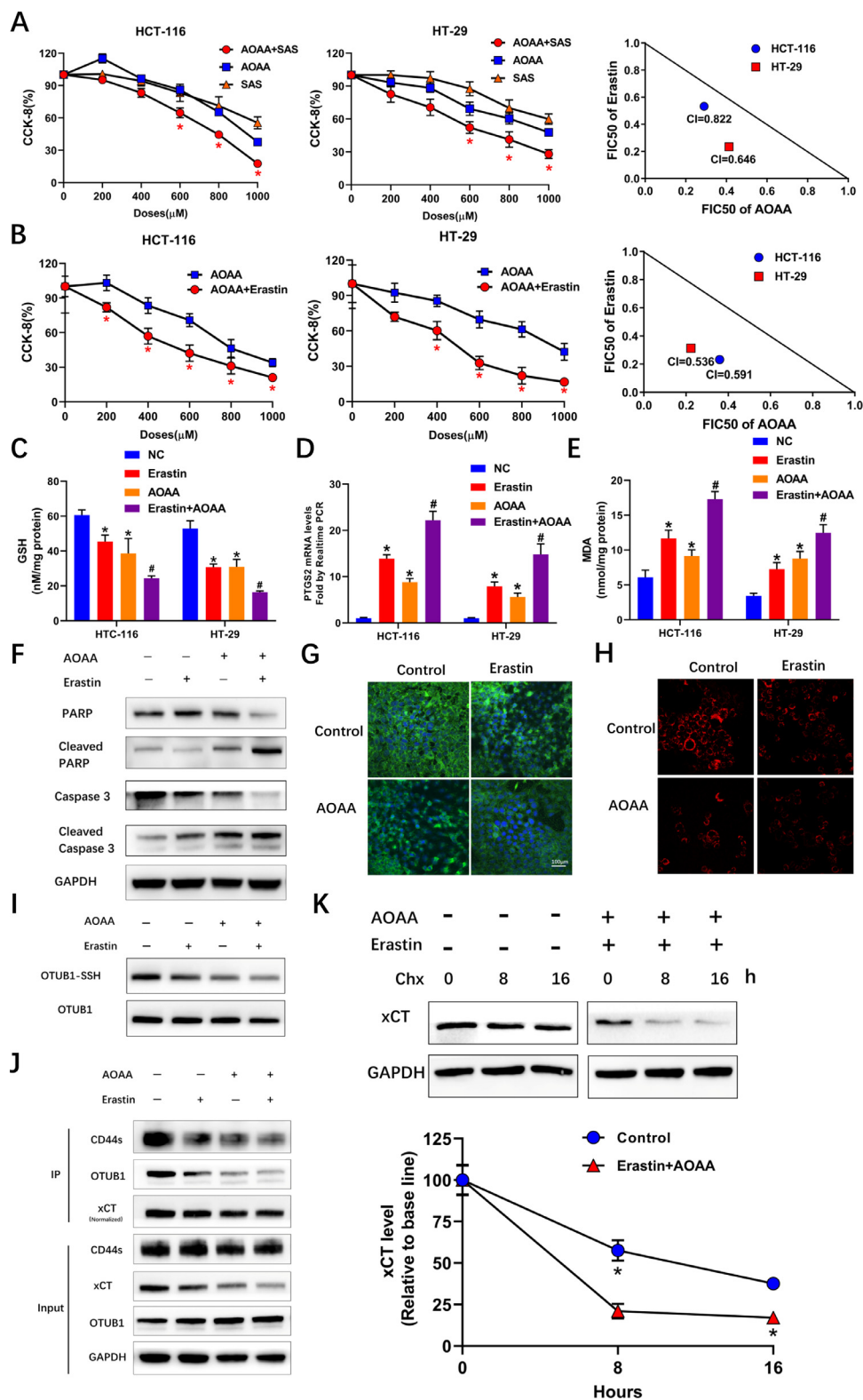
Fig. 4. Synthetic lethality of combing AOAA with SAS or Erastin. (A) CCK-8 assays showing increased lethality induced by AOAA+SAS compared with either alone in HCT-116 and HT-29 cells and isobologram indicating a synergistic effect of AOAA+SAS in both cell lines. In left middle panels, x axis indicated doses used for both AOAA and SAS. (*P < 0.05 vs either alone). (B) CCK-8 assays showing increased lethality induced by AOAA+Erastin compared with either alone in HCT-116 and HT-29 cells and isobologram indicating a synergistic effect of AOAA+Erastin in both cell lines. In left and middle panels, x axis indicated doses used for AOAA with Erastin at a fixed dose (5μM for both cell lines). (*P < 0.05 vs either alone). (C) Combining Erastin and AOAA induced further decreased intracellular GSH levels in both cell lines. (D) Quantitative real-time PCR showing that combining Erastin and AOAA induced further increased PTGS2 mRNA levels in both cell lines. (E) Combining Erastin and AOAA induced further increased MDA levels in both cell lines. (* P < 0.05 vs negative control[NC], #P < 0.05 vs either AOAA or Erastin alone groups). (F) Immunoblots showing increased cleavage of PARP and Caspase 3 after combing AOAA and Erastin in HCT-116 cells. (G) IF showing drastically deceased intensity of xCT after combining AOAA and Erastin in HCT-116 cells. (H) Further decreased H$_2$S levels in HCT-116 cells treated with the combination of AOAA and Erastin. (I) Modified biotin switch assays indicating decreased persulfidation induced by AOAA and Erastin alone and further decreased persulfidation induced by combination. (J) Immunoblots following IP
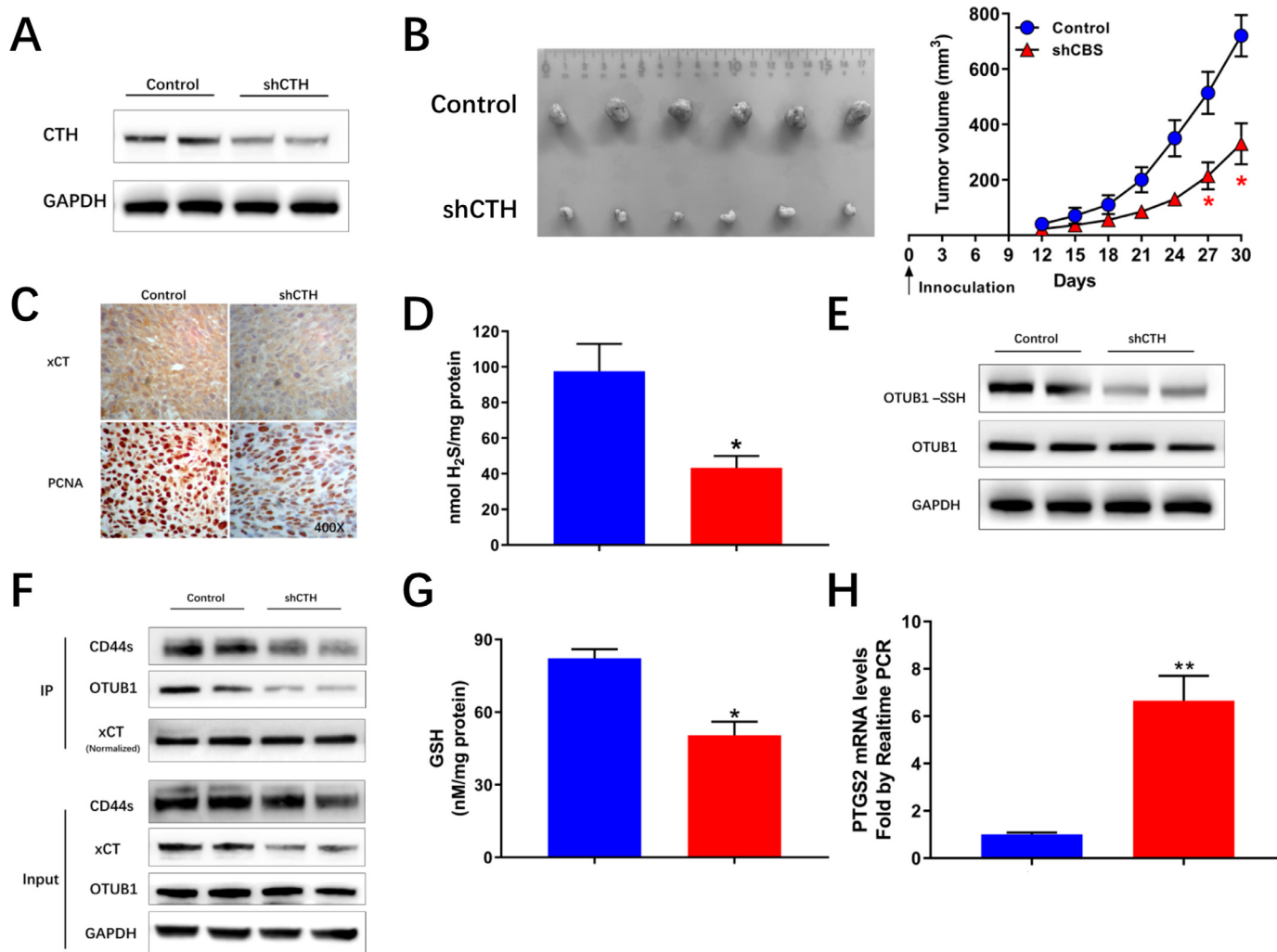
Fig. 5. Inhibiting CTH decreases xCT stability in vivo. (A) Immunoblots showing decreased CTH expression in HCT-116 shCTH cells. (B) Mice injected with shCTH cell lines exhibited decreased tumor volume compared with control animals injected with HCT-116 cell lines transfected with negative control plasmids. (C) IHC images showing decreased xCT and Ki67 intensity in shCTH tumors. (D) Decreased H_2S levels in shCTH tumors. (E) Modified biotin switch assays showing decreased persulfidation of OTUB1 in shCTH tumors. (F) Immunoblots following IP showing decreased xCT levels and decreased conjunction between OTUB1 and xCT in shCTH tumors. (G) Decreased GSH levels in shCTH tumors. (H) Quantitative real-time PCR showing increased PTGS2 mRNA levels in shCTH tumors. (*$P < 0.05$ vs Control).

xCT levels and decreased conjunction between xCT and OTUB1 (Fig. 5F). Decreased GSH levels and increased ferroptosis, featured by increased mRNA levels of PTGS2 (Figs 5G and H) was validated in shCTH groups.

The synthetic lethality of combining AOAA and Erastin was further validated *in vivo*. The results indicated that this combination resulted in significant inhibition of tumor growth (Fig. 6A), as well as a further decreased H_2S levels and persulfidation of OTUB1 (Fig. 6B and C). Reduced xCT levels and decreased conjunction of OTUB1 with xCT was also evident in the group of combination (Fig. 6D). This combination also resulted in significantly increased ferroptosis, featured by increased mRNA levels of PTGS and increased MDA levels (Fig. 6E and F).

Discussion

xCT, aka SLC7A11, is the functional subunit of system Xc-, a cysteine-glutamate antiporter, which provides substrate for synthesis of GSH [27]. Increased expression of xCT has been validated in multiple types of cancer including CRC [28,29]. Accumulating studies have recognized xCT as a

critical nexus of linking anti-oxidation and metabolic reprogramming of cancer cells [30]. Very recently, a close relationship between xCT and ferroptosis, a newly recognized, iron-dependent form of cell death, has been revealed [31]. Suppression of xCT was a major contributor to ferroptotic cell death induced by both radiotherapy and immunotherapy [32]. The proper function of the tumor suppressor molecule p53 also relied on inhibiting xCT [33]. However, despite the fact of increased xCT levels in CRC and multiple mechanisms revealed underlying the inhibition of xCT potentiated by therapeutic approaches and tumor suppressor genes, the mechanisms maintaining the elevated xCT levels in tumor cells especially in the challenge of treatment remain largely elusive. We observed that xCT was overexpressed in CRC and further increased expression was illustrated in LM and cell lines with resistance to 5-FU. Interfering xCT resulted in increased expression of CTH and CBS, which were major components of the transsulfuration pathway. Besides, interfering xCT significantly decreased endogenous H_2S levels. While, supplementation of H_2S with GYY4137 saved the loss of resistance to 5-FU induced by xCT interfering, demonstrating a functional role of H_2S in mediating the effect of xCT in maintaining chemoresistance.
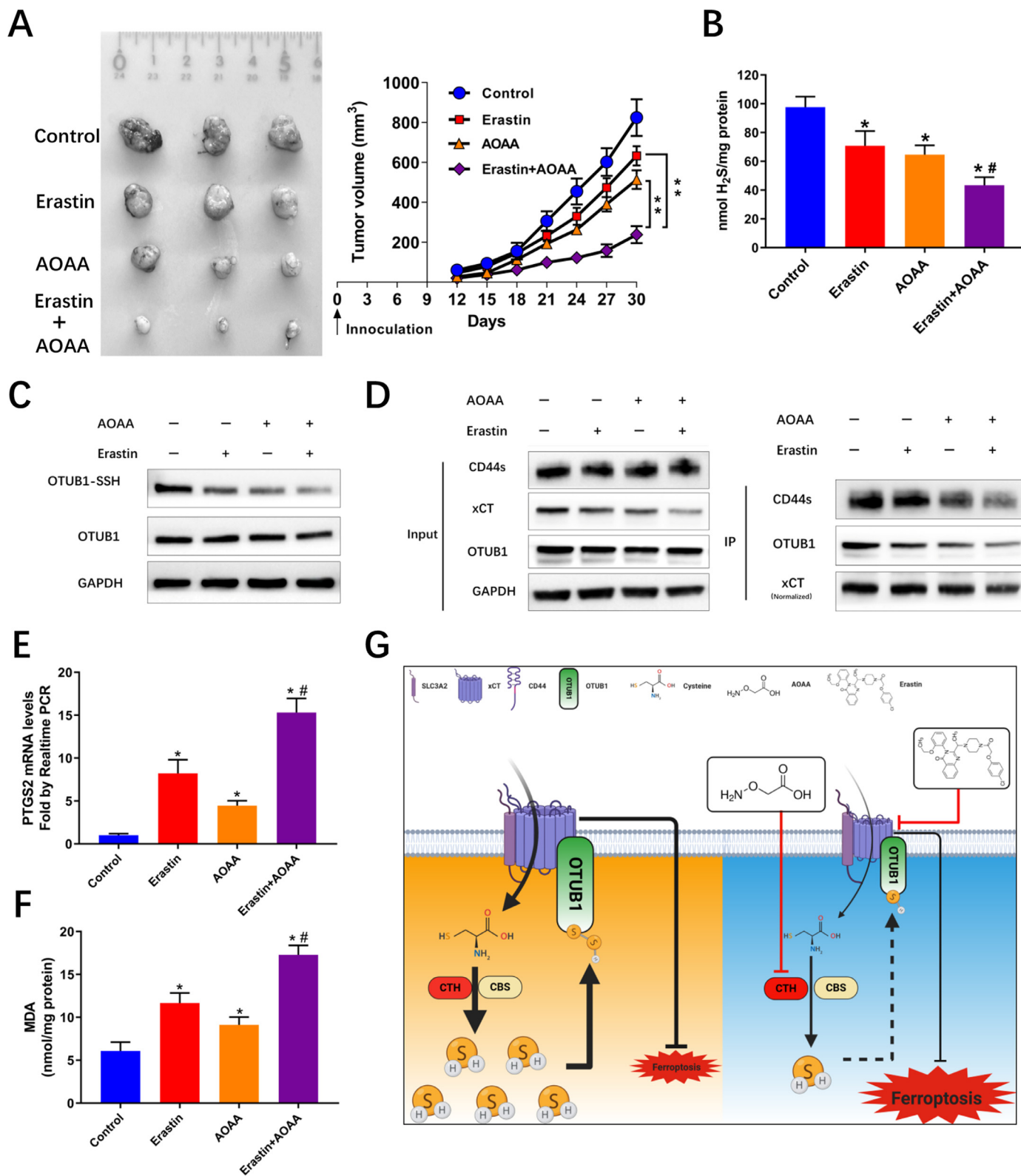
Fig. 6. Synthetic lethality and regulation of xCT stability of H_2S mediated persulfidation of OTUB1 *in vivo*. (A) Combined treatment with AOAA and Erastin resulted in further decreased tumor volume compared with either alone. (**$P < 0.01$) (B) Combination of AOAA and Erastin induced further decreased H_2S levels in tumors. (*$P < 0.05$ vs Control, #$P < 0.05$ vs either Erastin or AOAA alone). (C) Combination induced further decreased persulfidation of OTUB1 in tumor cells. (D) Combination induced further decreased xCT levels and conjunction between OTUB1 and xCT. (E) and (F) Combination of AOAA induced further increased PTGS2 mRNA and MDA levels in tumors. (*$P < 0.05$ vs Control, #$P < 0.05$ vs either Erastin or AOAA alone). (G) Schematic diagram showing reciprocal regulation between xCT stability and the transsulfuration pathway before and after combined blocking with AOAA and Erastin.

Strikingly, CTH-H$_2$S increased the steady state xCT protein levels without significant influence on xCT mRNA levels. These results led us to investigate the potential post-translational regulatory effect of H$_2$S on xCT levels.

Persulfidation of specific cysteine residues has been involved in the post-translational modification of multiple proteins mediated by endogenous H$_2$S. Both enhancement and attenuation of the function of proteins could be resulted by persulfidation in a context specific manner [34,35]. Modified biotin switch assays were widely adopted to detect the persulfidation levels of proteins utilizing specific antibodies [36]. OTUB1 is a deubiquitinating enzyme that promotes protein stabilization through unconventional mechanisms [37,38]. Recent studies revealed that overexpressed OTUB1 promotes tumor development by stabilizing xCT through direct conjunction [24]. We investigated the potential regulation of OTUB1 persulfidation mediated by CTH-H$_2$S axis. Intriguingly, persulfidation of OTUB1 and its conjunction with xCT was closely related with endogenous H$_2$S levels. To delineate the cysteine residue accounted for the effect of H$_2$S on the binding of OTUB1 with xCT. OTUB1 expressing plasmids with point mutations from cysteine to alanine were constructed respectively in correspondence to the 4 cysteine residues (C23, C91, C204, C212) in OTUB1 amino acid sequence. The results indicated that neither one of these mutations abrogated the persulfidation of OTUB1 exerted by H$_2$S. However, C91A plasmids abrogated the increased xCT levels induced by H$_2$S. Besides, C91A also prevented the increased conjunction between OTUB1 and xCT potentiated by H$_2$S. Previous studies suggested that point mutation in C91 to alanine fully retains the ability of OTUB1 to stabilize the target proteins including xCT, which ruled out the influence of the potential change of OTUB1 function caused by this point mutation [24,39]. Together, these results indicated that CTH-H$_2$S axis maintains the stability of xCT through persulfidation of OTUB1 at cysteine 91.

Ferroptosis is a newly recognized form of cell death, feature by lipid peroxidation, which has been related with the therapeutic effects and mechanism of radiation, chemotherapeutic reagents and most importantly checkpoint inhibitors based immune therapy [40−42]. Both transsulfuration pathway and xCT have been confirmed to be regulators of ferroptosis in cancer cells, mainly through providing cysteine as substrates for the synthesis of GSH, the dominant antioxidants [7,10]. Based on the previous reports and our results, we set out to investigate the potential of combine blocking of xCT and the transsulfuration pathway. Interestingly, synergistic effect was revealed between AOAA, an inhibitor of CBS and CTH, with SAS and Erastin in inhibiting the viability of colon cancer cells. The combination of AOAA and Erastin resulted in further decreased intracellular GSH levels and consequently increased ferroptosis, characterized by increased PTGS2 mRNA levels and MDA, the end product of lipid oxidation [43,44]. Considering the central role of reactive oxygen species in inducing apoptosis in canner cells, we further analyzed apoptosis induced by this combination and found that increased apoptosis also contributed to the synthetic lethality induced by this combination [45]. Besides, further decreased xCT levels and endogenous H$_2$S levels were induced by this combination. Together, these results suggested that the decreased persulfidation of OTUB1 resulting from the inhibited H$_2$S levels led to drastically decreased stabilization of xCT protein levels through attenuation of its binding with xCT.

Finally, we set out to investigate the persulfidation of OTUB1 and the synthetic lethality of combing AOAA and Erastin *in vivo*. The results indicated that inhibiting CTH expression significantly truncated the proliferation of tumor xenografts. Decreased expression of xCT and persulfidation of OTUB1 was evident in shCTH tumors. Besides, inhibiting CTH resulted in decreased tumor derived H$_2$S as well as intracellular GSH levels, accompanied by increased ferroptosis, featured by increased PTGS2 mRNA levels. Xenograft models further supported the synthetic lethality of combining AOAA and Erastin. The decreased xCT levels and persulfidation mediated regulation of OTUB1 binding with xCT was also validated *in vivo*.

Our present study revealed a reciprocal regulation between xCT and the endogenous H$_2$S derived from the transsulfuration pathway. Cystine, imported by xCT, provided substrate for the production of H$_2$S through the transsulfuration pathway, which was composed of rate limiting enzymes including CBS and CTH [46]. On the other hand, the transsulfuration pathway-H$_2$S axis (mainly CTH-H$_2$S axis) stabilized the xCT through persulfidation of OTUB1. This reciprocal regulation created a targetable vulnerability in the metabolic reprogramming of cancer. Indeed, combining AOAA and Erastin induced synthetic lethality in colon cancer cells, accompanied with increased ferroptosis and apoptosis elicited by intracellular oxidation crisis created by this combination.

Overall, our findings suggest that a reciprocal regulation exists between xCT and endogenous H$_2$S levels. H$_2$S maintains the stability of xCT via persulfidation of OTUB1 at Cysteine 91. Combined blocking with AOAA and Erastin resulted in synthetic lethality which was mediated mainly through induction of ferroptosis (Fig. 6G).

Author contributions

Conceptualization and design: SC, WP. Methodology: SC, DB, JZ, TY. Acquisition of data: SC, XW. Writing, review of the manuscript: SC, YP, YL, PW. Both SC and XW were aware of the group allocation of the animal experiment. -2

Ethics approval and consent to participate

All animal experiments have been approved by the Institutional review board at Peking University First Hospital, Beijing, China.

Consent for publication

All authors have agreed to publish this manuscript.

Data availability

The data generated and analyzed in this study are available from the corresponding author on reasonable request.

Acknowledgements

Supplementary materials

Supplementary material associated with this article can be found, in the online version, at doi:10.1016/j.neo.2021.03.009.

References

1 Siegel RL, Miller KD, Goding Sauer A, Fedewa SA, Butterly LF, Anderson JC, Cercek A, Smith RA, Jemal A. Colorectal cancer statistics, 2020. *CA Cancer J Clin* 2020;**70**(3):145–64.

2 Liu J, Xia X, xCT Huang P. A critical molecule that links cancer metabolism to redox signaling. *Mol Ther* 2020;**28**(11):2358–66.

3 Daher B, Parks SK, Durivault J, Cormerais Y, Baidarjad H, Tambutte E, Pouysségur J, Vučetić M. Genetic ablation of the cystine transporter xCT in PDAC cells inhibits mTORC1, growth, survival, and tumor formation via nutrient and oxidative stresses. *Cancer Res* 2019;**79**(15):3877–90.

4 Shin CS, Mishra P, Watrous JD, Carelli V, D'Aurelio M, Jain M, Chan DC. The glutamate/cystine xCT antiporter antagonizes glutamine metabolism and reduces nutrient flexibility. *Nat Commun* 2017;**8**:15074.

5 Conti L, Bolli E, Di Lorenzo A, Franceschi V, Macchi F, Riccardo F, Ruiu R, Russo L, Quaglino E, Donofrio G, Cavallo F. Immunotargeting of the xCT cystine/glutamate antiporter potentiates the efficacy of HER2-targeted immunotherapies in breast cancer. *Cancer Immunol Res* 2020;**8**(8):1039–53.

6 Stockwell BR, Friedmann Angeli JP, Bayir H, Bush AI, Conrad M, Dixon SJ, Fulda S, Gascón S, Hatzios SK, Kagan VE, et al.. Ferroptosis: A Regulated Cell Death Nexus Linking Metabolism, Redox Biology, and Disease, 171. Cell; 2017. p. 273–85.

7 Koppula P, Zhuang L, Gan B. Cystine transporter SLC7A11/xCT in cancer: ferroptosis, nutrient dependency, and cancer therapy. *Protein Cell* 2020 Online ahead of print. doi:10.1007/s13238-020-00789-5.

8 Liu N, Lin X, Huang C. Activation of the reverse transsulfuration pathway through NRF2/CBS confers erastin-induced ferroptosis resistance. *Br J Cancer* 2020;**122**(2):279–92.

9 Weber R, Birsoy K. The transsulfuration pathway makes, the tumor takes. *Cell Metab* 2019;**30**(5):845–6.

10 Wang L, Cai H, Hu Y, Liu F, Huang S, Zhou Y, Yu J, Xu J, Wu F. A pharmacological probe identifies cystathionine beta-synthase as a new negative regulator for ferroptosis. *Cell Death Dis* 2018;**9**(10):1005.

11 Wang M, Mao C, Ouyang L, Liu Y, Lai W, Liu N, Shi Y, Chen L, Xiao D, Yu F, et al. Long noncoding RNA LINC00336 inhibits ferroptosis in lung cancer by functioning as a competing endogenous RNA. *Cell Death Differ* 2019;**26**(11):2329–43.

12 Hine C, Harputlugil E, Zhang Y, Ruckenstuhl C, Lee BC, Brace L, Longchamp A, Treviño-Villarreal JH, Mejia P, Keith Ozaki C, et al. Endogenous hydrogen sulfide production is essential for dietary restriction benefits. *Cell* 2015;**160**(1-2):132–44.

13 Szabo C, Coletta C, Chao C, Módis K, Szczesny B, Papapetropoulos A, Hellmich MR. Tumor-derived hydrogen sulfide, produced by cystathionine-beta-synthase, stimulates bioenergetics, cell proliferation, and angiogenesis in colon cancer. *Proc Natl Acad Sci U S A* 2013;**110**(30):12474–9.

14 Szabo C. Gasotransmitters in cancer: from pathophysiology to experimental therapy. *Nat Rev Drug Discov* 2016;**15**(3):185–203.

15 Zhao S, Song T, Gu Y, Zhang Y, Cao S, Miao Q, Zhang X, Chen H, Gao Y, Zhang L, et al. Hydrogen sulfide alleviates liver injury via S-sulfhydrated-Keap1/Nrf2/LRP1 pathway. *Hepatology* 2020 Online ahead of print. doi:10.1002/hep.31247.

16 Cui C, Fan J, Zeng Q, Cai J, Chen Y, Chen Z, Wang W, Li SY, Cui Q, Yang J, et al. CD4(+) T-cell endogenous cystathionine gamma lyase-hydrogen sulfide attenuates hypertension by sulfhydrating liver kinase B1 to promote T regulatory cell differentiation and proliferation. *Circulation* 2020;**142**(18):1752–69.

17 Zhang K, Zhang J, Xi Z, Li LY, Gu X, Zhang QZ, Yi L. A new H(2)S-specific near-infrared fluorescence-enhanced probe that can visualize the H(2)S level in colorectal cancer cells in mice. *Chem Sci* 2017;**8**(4):2776–81.

18 d'Emmanuele di Villa Bianca R, Mitidieri E, Di Minno MN, Kirkby NS, Warner TD, Di Minno G, Cirino G, Sorrentino R. Hydrogen sulphide pathway contributes to the enhanced human platelet aggregation in hyperhomocysteinemia. *Proc Natl Acad Sci U S A.* 2013;**110**(39):15812–17.

19 Chou TC. Drug combination studies and their synergy quantification using the Chou-Talalay method. *Cancer Res* 2010;**70**(2):440–6.

20 Högel H, Miikkulainen P, Bino L, Jaakkola PM. Hypoxia inducible prolyl hydroxylase PHD3 maintains carcinoma cell growth by decreasing the stability of p27. *Mol Cancer* 2015;**14**:143.

21 Yang R, Qu C, Zhou Y, Konkel JE, Shi S, Liu Y, Chen C, Liu S, Liu D, Chen Y, et al. Hydrogen sulfide promotes Tet1- and Tet2-mediated Foxp3 demethylation to drive regulatory T cell differentiation and maintain immune homeostasis. *Immunity* 2015;**43**(2):251–63.

22 Bansal A, Simon MC. Glutathione metabolism in cancer progression and treatment resistance. *J Cell Biol* 2018;**217**(7):2291–8.

23 Li L, Whiteman M, Guan YY, Neo KL, Cheng Y, Lee SW, Zhao Y, Baskar R, Tan C-H, Moore PK, et al. Characterization of a novel, water-soluble hydrogen sulfide-releasing molecule (GYY4137): new insights into the biology of hydrogen sulfide. *Circulation* 2008;**117**(18):2351–60.

24 Filipovic MR, Zivanovic J, Alvarez B, Banerjee R. Chemical biology of H(2)S signaling through persulfidation. *Chem Rev* 2018;**118**(3):1253–337.

25 Liu T, Jiang L, Tavana O, Gu W. The deubiquitylase OTUB1 mediates ferroptosis via stabilization of SLC7A11. *Cancer Res* 2019;**79**(8):1913–24.

26 Asimakopoulou A, Panopoulos P, Chasapis CT, Coletta C, Zhou Z, Cirino G, Giannis A, Szabo C, Spyroulias GA, Papapetropoulos A. Selectivity of commonly used pharmacological inhibitors for cystathionine beta synthase (CBS) and cystathionine gamma lyase (CSE). *Br J Pharmacol* 2013;**169**(4):922–32.

27 Bridges R, Lutgen V, Lobner D, Baker DA. Thinking outside the cleft to understand synaptic activity: contribution of the cystine-glutamate antiporter (System xc-) to normal and pathological glutamatergic signaling. *Pharmacol Rev* 2012;**64**(3):780–802.

28 Hu K, Li K, Lv J, Feng J, Chen J. Suppression of the SLC7A11/glutathione axis causes synthetic lethality in KRAS-mutant lung adenocarcinoma. *J Clin Invest* 2020;**130**(4):1752–66.

29 Bhutia YD, Babu E, Ramachandran S, Ganapathy V. Amino acid transporters in cancer and their relevance to "glutamine addiction": novel targets for the design of a new class of anticancer drugs. *Cancer Res* 2015;**75**(9):1782–8.

30 Lin W, Wang C, Liu G, Bi C, Wang X, Zhou Q, Jin H. SLC7A11/xCT in cancer: biological functions and therapeutic implications. *Am J Cancer Res* 2020;**10**(10):3106–26.

31 Xie Y, Hou W, Song X, Yu Y, Huang J, Sun X, Kang R, Tang D. Ferroptosis: process and function. *Cell Death Differ* 2016;**23**(3):369–79.

32 Lang X, Green MD, Wang W, Yu J, Choi JE, Jiang L, Liao P, Zhou J, Zhang Q, Dow A, et al. Radiotherapy and immunotherapy promote tumoral lipid oxidation and ferroptosis via synergistic repression of SLC7A11. *Cancer Discov* 2019;**9**(12):1673–85.

33 Jiang L, Kon N, Li T, Wang SJ, Su T, Hibshoosh H, Baer R, Gu W. Ferroptosis as a p53-mediated activity during tumour suppression. *Nature* 2015;**520**(7545):57–62.

34 Zivanovic J, Kouroussis E, Kohl JB, Adhikari B, Bursac B, et al. Selective persulfide detection reveals evolutionarily conserved antiaging effects of S-sulfhydration. *Cell Metab* 2019;**30**(6):1152–70.

35 Paul BD, Snyder SH. H2S: a novel gasotransmitter that signals by sulfhydration. *Trends Biochem Sci* 2015;**40**(11):687–700.

36 Meng G, Zhao S, Xie L, Han Y, Ji Y. Protein S-sulfhydration by hydrogen sulfide in cardiovascular system. *Br J Pharmacol* 2018;**175**(8):1146–56.

37 Nakada S, Tai I, Panier S, Al-Hakim A, Iemura S-I, Juang Y-C, O'Donnell L, Kumakubo A, Munro M, Sicheri F, et al. Noncanonical inhibition of DNA damage-dependent ubiquitination by OTUB1. *Nature* 2010;**466**:941–6.

38 Wiener R, Zhang X, Wang T, Wolberger C. The mechanism of OTUB1-mediated inhibition of ubiquitination. *Nature* 2012;**483**(7391):618–22.

39 Juang Y-C, Landry M-C, Sanches M, Vittal V, Leung CCY, Ceccarelli DF, Mateo A-RF, Pruneda JN, Mao DYL, Szilard RK, et al. OTUB1 co-opts Lys48-linked ubiquitin recognition to suppress E2 enzyme function. *Mol Cell* 2012;**45**:384–97.

40 Lei G, Zhang Y, Koppula P, Liu X, Zhang J, Lin SH, Ajani JA, Xiao Q, Liao Z, Wang H, et al. The role of ferroptosis in ionizing radiation-induced cell death and tumor suppression. *Cell Res* 2020;**30**(2):146–62.

41 Friedmann Angeli JP, Krysko DV, Conrad M. Ferroptosis at the crossroads of cancer-acquired drug resistance and immune evasion. *Nat Rev Cancer* 2019;**19**(7):405–14.

42 Wang W, Green M, Choi JE, Gijón M, Kennedy PD, Johnson JK, Liao P, Lang X, Kryczek I, Sell A, et al. CD8(+) T cells regulate tumour ferroptosis during cancer immunotherapy. *Nature* 2019;**569**(7755):270–4.

43 Yang WS, SriRamaratnam R, Welsch ME, Shimada K, Skouta R, Viswanathan VS, Cheah JH, Clemons PA, Shamji AF, Clish CB, et al. Regulation of ferroptotic cancer cell death by GPX4. *Cell* 2014;**156**:317–31.

44 Marrocco I, Altieri F, Peluso I. Measurement and clinical significance of biomarkers of oxidative stress in humans. *Oxid Med Cell Longev* 2017;**2017**:6501046.

45 Cui Q, Wang JQ, Assaraf YG, Ren L, Gupta P, Wei L, Ashby CR Jr, Yang DH, Chen ZS. Modulating ROS to overcome multidrug resistance in cancer. *Drug Resist Updat* 2018;**41**:1–25.

46 Sbodio JI, Snyder SH, Paul BD. Regulators of the transsulfuration pathway. *Br J Pharmacol* 2019;**176**(4):583–93.